# Multipolar scattering of subwavelength interacting particles: Extraction of effective properties between transverse and longitudinal optical modes

Cédric Blanchard,[1,*] Jean-Paul Hugonin,[2] Alima Nzie,[1] and Domingos De Sousa Meneses[1]
[1]*CNRS, CEMHTI UPR3079, Univ. Orléans, F-45071 Orléans, France*
[2]*Laboratoire Charles Fabry, Institut d'Optique Graduate School, CNRS, Université Paris-Saclay, 91127 Palaiseau, France*

(Received 1 April 2020; revised 20 June 2020; accepted 4 August 2020; published 18 August 2020)

The general concern of this investigation is the extraction of the effective electromagnetic properties of agglomerates of randomly located particles, which are small compared to the wavelength. The focus is on the spectral window ranging from the transverse phonon to the longitudinal phonon frequencies, in which resonances may be excited. In this frequency domain, it is shown that limiting the problem to bare dipole-dipole interactions leads to inaccurate calculations of the electromagnetic fields, resulting in a doubtful extraction of the effective properties. We perform the complete electromagnetic calculation by taking into account the higher multipole orders that are activated when the agglomerates are illuminated. Several results, which are not usually observed outside the frequency range highlighted here, are revealed by means of extensive numerical simulations. In particular, we evidence large deviations compared to the predictions provided by the effective medium theories, while we find that the volume of the microstructures (each one with a different internal geometry) that are used to average the fields must be unusually large to avoid a bias in the determination of the effective properties. Furthermore, the evolution of the incoherent component of the fields between the two optical phonon modes is investigated.

DOI: 10.1103/PhysRevB.102.064209

## I. INTRODUCTION

The conceptual and fundamental issue of determining the effective refractive index of inhomogeneous media has attracted the attention of the scientific community for long; early quantitative discussions on this topic turn out to date back to the first part of the 19th century [1]. From a practical viewpoint, the knowledge of the effective refractive index $n_{\text{eff}}$ provides useful information, for example in the realm of heat transfer or in the propagation of light in random media, where its imaginary part is directly related to the absorption coefficient appearing in the radiative transfer equation or in the Beer-Lambert law. There is a wide range of applications lying in the determination of $n_{\text{eff}}$, e.g., characterization of industrial nanopowders [2] or colloids [3], thermoradiative properties of foams for solar absorbers [4], etc.

Several predicting models with different level of sophistication exist. Let us mention the well-known Maxwell-Garnett (MG) [5] and Bruggeman [6] models, which are two formulas expressing the effective permittivity ($\epsilon_{\text{eff}} = n_{\text{eff}}^2$) of a mixture in terms of the relative permittivities and volume fractions of the bare components. However, these last two quantities are in general insufficient to correctly describe the effective properties of a mixture. Accordingly, other approximation methods that take into account further inputs, such as microstructural information [7], were developed. Another approach lies in the computation of the electromagnetic fields and in the obtention of the effective parameters by means of different techniques: e.g., (i) using the formula $\epsilon_{\text{eff}} = \langle \mathbf{D} \rangle / \langle \mathbf{E} \rangle$ where $\mathbf{E}$ and $\mathbf{D}$ are the electric and displacement fields, averaged over a volume that is representative of the inhomogeneous medium under study [8], (ii) averaging the electromagnetic field scattered by many spherical agglomerates (in all the realizations, the volume fraction is maintained constant while the position of the particles is varied) and comparing with the response of a homogeneous sphere for which the scattered field is provided by Mie's theory [9], or (iii) calculating the reflection and transmission coefficients of an inhomogeneous slab consisting of a distribution of particles and comparing with the analytical coefficients that hold for a homogeneous slab [10].

The diffraction of an electromagnetic radiation by a single particle is a classic problem. So long as the size of the particle remains small compared to the wavelength, the diffracted field reduces to the first-order component of the expansion in terms of the vector spherical wave functions. In this case and if the host media is free space, it should be noted that the formula giving the oscillation amplitude exhibits a pole when the permittivity of the particle takes the value $\epsilon_p = -2$ [11]. The particle experiences surface plasmon polariton resonances and the frequency at which this occurs is called the Fröhlich frequency $\omega_F$ [12], accordingly given by $\epsilon_p(\omega_F) = -2$.

The case where two particles are involved provides an interesting simplified frame to understand the collective effects that may arise. This problem was largely investigated in the past, many contributions [13–15] are based on a $T$-matrix kind approach, which lies in a multipole expansion of the field around the scatterers and in the addition theorem that allows us to express the spherical harmonics about one origin in terms of those at other origins.

*Corresponding author: cedric.blanchard@cnrs-orleans.fr

 

While the assumption of a dipole-dipole interaction is often made when the particles are small compared to the wavelength [16,17], it was shown that higher-order multipoles are actually required as the clearance decreases, especially when the particles have a large refractive index [13] or when surface plasmon polariton resonances are excited [18]. In the latter case, the Fröhlich's mode splits into several resonant modes whose eigenfrequencies depend on the interparticle distance.

The number of multipolar modes that are activated when an agglomerate is illuminated is a prominent issue because the computational burden can become impracticable if the cluster is made up of many particles and if high-order multipoles are simultaneously required. Furthermore, the multipolar collective response of the cluster seems to be incompatible with some effective medium theories such as MG, which is usually understood as a single scattering model with no multiple-scattering interactions between the constitutive dipoles [19]. Therefore, the widely held assumption that MG is accurate in predicting $n_{\text{eff}}$ for clusters with a low concentration of spherical particles runs counterintuitive with the fact that several multipole orders may be necessary. The deviation of the effective permittivity in regard to MG in those situations in which the mixing rule model should at first glance work is a question that will be, in particular, addressed here.

In this work, we focus on the spectral range bounded by the transverse frequency $\omega_{TO}$ and the longitudinal frequency $\omega_{LO}$ of an optical phonon mode. We will evidence unconventional effective behaviors in this frequency range.

Section II is a brief summary in which the $\omega_{TO}$-$\omega_{LO}$ range is discussed. In Sec. III, we show that a many-particle agglomerate experiences strong resonances in a large portion of the $\omega_{TO}$-$\omega_{LO}$ domain. We verify, for large clouds of scatterers, that at the edge of the resonant spectrum the electromagnetic interactions are contained into the higher-order multipoles [20]. We investigate the role of the clearance between the particles, and we show that it is mainly through this parameter that the bandwidth of the resonant region is driven.

Next, we extract the effective properties of inhomogeneous materials through an ensemble average over a great number of realizations, each one with a different spatial distribution of the particles. We demonstrate in Sec. IV that, even in the single-scattering approximation, MG can fail in predicting the effective properties in the $\omega_{TO}$-$\omega_{LO}$ range. In Sec. V, the collective effects are taken into account by activating the multipolar interactions. We establish that the power scattered by the constitutive realizations of the ensemble average displays strong fluctuations between each other. We show that the incoherent part of the fields does not only originate from the random positions of the scatterers in the finite agglomerates but also from electromagnetic interactions. More specifically, it is evidenced that the incoherent effects gradually increase while entering the core of the $\omega_{TO}$-$\omega_{LO}$ range, up to a limit from which strong resonances appear. As a consequence, the calculated $n_{\text{eff}}$ can significantly deviate from MG or can even be impossible to determine. By means of statistical considerations, it will be pointed out that the volume and number of the realizations in the ensemble average should be carefully adjusted. Insufficiently large volumes lead to a bias in the calculated $n_{\text{eff}}$ and require a great number of realizations; we find that this effect is dramatically enhanced compared to what is observed outside the $\omega_{TO}$-$\omega_{LO}$ domain and, what is more, it strongly depends on the refractive index of the particles.

## II. TRANSVERSE AND LONGITUDINAL OPTICAL PHONON MODES

Phonons in crystals are normal modes of vibration that can cause strong interactions between electromagnetic fields and matter in the far- and midinfrared ranges. If their symmetry satisfies the selection rules for infrared activity, there is a large dielectric dispersion around their resonant frequencies, which induces the presence of characteristic bands in the reflectivity spectrum of the material. In the spectral domain where strong interactions occur, the electric response is fairly well described by a four-parameter dielectric function model whose expression is given by [21]:

$$\epsilon(\omega) = \epsilon_r(\omega) + i\epsilon_i(\omega) = \epsilon_\infty \prod_j \frac{\omega_{jLO}^2 - \omega^2 - i\gamma_{jLO}\omega}{\omega_{jTO}^2 - \omega^2 - i\gamma_{jTO}\omega}. \quad (1)$$

Four parameters are necessary to take into account the contribution of each phonon. The frequencies $(\omega_{jTO}, \omega_{jLO})$ and the dampings $(\gamma_{jTO}, \gamma_{jLO})$ are characteristics of the transverse $(TO)$ and longitudinal optic $(LO)$ modes associated with the $j$th phonon term. The permittivity $\epsilon_\infty = 1 + \chi_\infty$ includes a high-frequency contribution due to valence electrons. For a hypothetic dielectric material having only one undamped phonon $(\gamma_{jTO} = \gamma_{jLO} = 0)$ and no high-frequency contribution $(\epsilon_\infty = 1)$, the previous expression reduces to:

$$\epsilon_r(\omega) = \frac{\omega_{LO}^2 - \omega^2}{\omega_{TO}^2 - \omega^2}, \quad (2a)$$

$$\epsilon_i(\omega) = \frac{\pi\left(\omega_{LO}^2 - \omega_{TO}^2\right)}{2\omega_{TO}}[\delta(\omega - \omega_{TO}) - \delta(\omega + \omega_{TO})], \quad (2b)$$

where $\delta$ represents the Dirac function. It is obvious from these expressions that the real part of the dielectric function becomes negative between $\omega_{TO}$ and $\omega_{LO}$. A specific study of this range is scientifically relevant since it includes the domain of frequencies for which sharp resonances are encountered in the scattering spectrum of dielectric or metallic aggregates. By taking $\omega_{TO} = 0$, the dielectric function expression reduces to the Drude model of free electrons with a plasma frequency $\omega_p$ equal to $\omega_{LO}$.

## III. SPECTRAL STUDY OF MANY-PARTICLE AGGLOMERATES

We start by generating an inhomogeneous large medium consisting of nonoverlapping particles that are randomly located. The volume fraction is enforced to be 14.8% while the radius of the particles is set at $r_p = 0.1$ $\mu$m. The resulting texture is displayed on the left side of Fig. 1. Next, a volume is extracted from the global medium by defining a spherical surface of radius $R$ and then selecting all the particles whose center lies in the bound of this sphere. In this paper, several volumes are considered; in order to give a picture of the resulting studied agglomerates, all of them are represented on the right-hand side of Fig. 1.

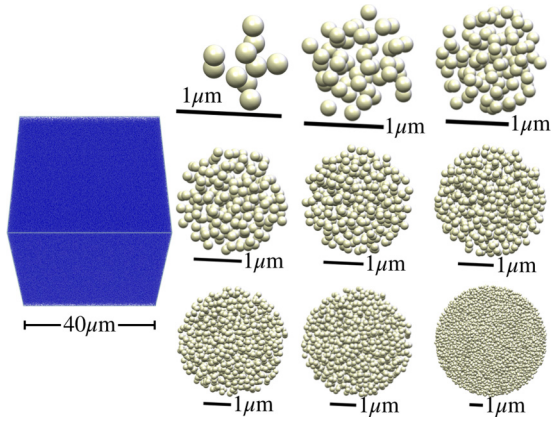


FIG. 1. The 40 $\mu$m × 40 $\mu$m (blue) sample is an inhomogeneous media. The constitutive particles are randomly positioned avoiding intersections, their radius is $r_p = 0.1$ $\mu$m, and the volume fraction is set at 14.8%. The numerical calculations are made on spherical volumes, extracted from the original sample, having different radii $R$. All the volumes used throughout this investigation are depicted here, from the top-left to bottom-right corners the radius is 0.4; 0.7; 0.85; 1.1; 1.3; 1.5; 1.9; 2; 4 $\mu$m.

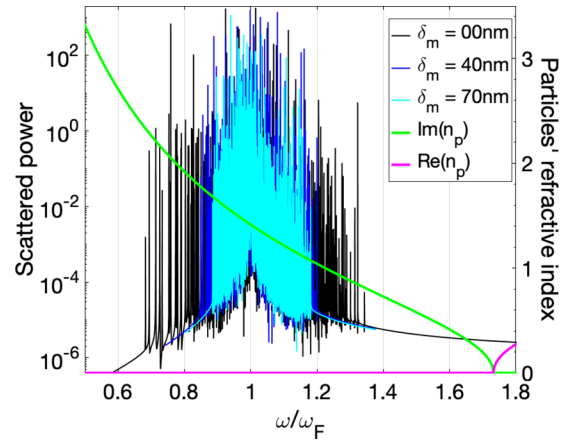


FIG. 2. Radiant flux for a random suspension of 90 particles in air against the frequency (normalized to the Fröhlich frequency). The minimum surface-to-surface distance between the particles is 0, 40, or 70 nm. The real and imaginary parts of the refractive index of the particles are also plotted.

We are interested in the bare electromagnetic response of a $R = 0.85$ $\mu$m cluster (corresponding to 90 particles) that is illuminated by a circularly polarized wave whose wavelength $\lambda$ is variable and much larger than the heterogeneities. While the polarization is often chosen in the literature to be of transverse electric (TE) or magnetic (TM) kind, we ensure a circular polarization in order to activate a greater number of modes in the cluster.

The dielectric constant of the particles is assumed to follow a Drude-type dispersion

$$\epsilon(\omega) = 1 - \frac{\omega_p^2}{\omega^2}, \tag{3}$$

where the plasma frequency is set at $\omega_p = 3.39 \times 10^{+13}\mathrm{s}^{-1}$.

Let us consider the black curve of Fig. 2, which corresponds to the case where there is no restriction on the minimum interparticle distance (i.e., a fully random medium disregarding the possibility of overlaps). One can observe the radiant power in terms of the frequency normalized to that of Frölich, which follows from Eq. (3). Sharp resonances in the scattering spectrum of the aggregate are clearly visible. These resonances originate from cooperative effects and result from the splitting of the Fröhlich's mode of a single particle. This phenomenon was discussed at length for aggregates made up of very few scatterers (e.g., Refs. [15,18]). It was in particular shown that as the number of particles increases, so does the number of resonances. Accordingly, the multiplicity of peaks in the spectrum of our rather large aggregate comes as no surprise, nonetheless to the best of our knowledge there are no studies dealing with the multipolar optical resonances of many-particle systems in the $\omega_{TO}$-$\omega_{LO}$ range.

The magenta and green curves plotted in Fig. 2 represent, respectively, the real and imaginary parts of $n_p$, the refractive index of the particles, which disperse according to Eq. (3). On the right-hand side of the figure, the axis has been labeled with the corresponding $n_p$ values. From this figure, it is straightforward to see the range of refractive indices that leads to strong resonances. Note that the $\omega_{TO}$-$\omega_{LO}$ range is characterized by a $n_p$ exhibiting a near zero real part.

The number of terms we retained in the multipole expansion is $L = 3$. At $L = 3$, the series is not well converged, this is here a deliberate choice, which allows us to sample the frequency interval in a thin manner (there are an amount of 75000 simulated points in the spectrum). Larger $L$ values were also tried, we found that $L = 20$ is not enough to get convergence. Because of computational limits (the calculations were realized with a 512 GB memory server), we were unable to go further in increasing $L$ and, at the same time, maintaining a reasonably large aggregate. However, we importantly noticed that the chief impact of increasing $L$ is to make larger the spectral interval exhibiting the resonances. It is worth emphasizing this result because it means that in the core of the $\omega_{TO}$-$\omega_{LO}$ range, resonant behaviors are likely to be revealed by high-order multipoles. As a result, the number of multipoles must be correctly sized up, otherwise resonant behaviors might be missed at given frequencies.

On the other hand, we simulated a $R = 2$ $\mu$m aggregate containing not less than 1190 particles; it was found that the resonant bandwidth is not impacted at all compared to the smaller aggregate so far investigated. By increasing $R$, the coefficient of variation, which we shall refer to as $C_V$ (often denominated as relative standard deviation), of the flux-vs-frequency data is reduced. However, such a reduction is quite modest; increasing the number of particles from 90 to 1190 only decreases $C_V$ by a factor of 2.

It should be noted that such statistical considerations have a tight relationship with the concept of representative volume element (RVE), which is basically defined as the smallest volume of the realizations that one must choose to ensure a statistical representativity of the texture under study. It was shown that the RVE size and the variance of a computed property of the realizations are related via the concept of range integral [22]. Therefore, the fact that $C_V$ slowly decreases poses the question of whether there exists a threshold for

the cluster volume above which it can be homogenized in the resonant regime, or even near resonance. Our attempt to apply the theory of range integral in the $\omega_{TO}$-$\omega_{LO}$ range was unsuccessful; the modest reduction of $C_V$ with the number of particles is incompatible with Kanit's power law in most of the spectral range we are interested in. This point is in agreement with studies asserting that homogenization can never be reached unless nonradiative losses are introduced into the particles [9].

Thus far, there is no constraint on the distance between the particles. Inasmuch as in many real disordered materials the inhomogeneities are not arbitrarily close from each other [23,24], it is interesting to investigate the impact on the electromagnetic behavior of the agglomerate if a minimum clearance is enforced. Note that outside the case $\delta_m = 0$, the medium cannot be considered as strictly random; for there is a forbidden volume of space where a given particle is not allowed to be located. In Fig. 2, we have plotted the spectrum of the scattered power for $\delta_m = 40\ \mu$m and $\delta_m = 70\ \mu$m. We observe a clear enlargement of the resonant window as $\delta_m$ is decreased. This result is a generalization of what is observed for a simple dimer in the dipolar and quadrupolar approximations [18] to a many-particle system where multiple modes are activated.

Another conclusion can be made regarding the single-scattering regime. We know that the scattering of the particles turns independent if $\delta_m$ is high enough, resulting in a single and sharp peak located at the Fröhlich frequency. However, the assertion high enough is quite vague. In opposition to what is often stated, we show here that interparticle distances comparable to the particle size may be outright insufficient to avoid collective effects, at least in a certain range of frequencies.

## IV. EFFECTIVE PROPERTIES OF CLUSTERS OF NONINTERACTING PARTICLES

Since it provides considerable simplification, single scattering is often assumed in the study of particle agglomerates [12]. In this case, the field scattered by the cluster is just obtained by summing over the field scattered by the individual particles. The single scattering regime plays a role in the context of the effective medium theories if one recognizes that the MG mixing rule can be derived by substituting the scatterers by dipoles with no interaction between each other [19]. Note in passing that the consensus is not entire on the physics behind MG; contradictorily, it is sometimes claimed that it is a first-order approximation accounting for dipole-dipole interactions [8].

The object of this section is to show that in a significant portion of the $\omega_{TO}$-$\omega_{LO}$ range, MG is unable to predict the effective properties of a suspension of noninteracting small particles. But let us start by presenting the technique that will be used along the whole paper to obtain the effective permittivities of the spherical agglomerates.

A large number of spherical clusters is illuminated by a circularly polarized plane wave. The clusters solely differ about the distribution of their constitutive particles, but all of them have the same volume fraction and the center of the particles belong to the same spherical volume of radius $R$. What is more, the wavelength is fixed at $\lambda = 100\ \mu$m, i.e., 1000 times larger than the radius of the constitutive particles. The scattering power is numerically calculated and collected for many directions around each one of the clusters (we sampled the three-dimensional space at more than 25000 solid angles), leading to 1000 different three-dimensional directional scattering patterns. We average them all together in order to extract a unique angular diagram. Once this is done, it only remains to use Mie's solution [11] to obtain the three-dimensional directional scattering pattern of a homogeneous sphere of radius $R$, which is then fitted to the numerically calculated data by the method of least squares. The refractive index of the homogeneous sphere that displays the same angular scattering pattern as the heterogeneous cluster is finally taken as the effective refractive index. It is worth pointing out that there can be several solutions to the problem, the existence of several branches is a classical issue in the theories of homogenization [25].

The MG model turns out to display a pole when the permittivity of the host medium $\epsilon_h$, the permittivity of the inclusions $\epsilon_p$, and the volume fraction $\Phi$ are such that $\epsilon_h(2 + \Phi) + \epsilon_p(1 - \Phi) = 0$ [26]. If $\epsilon_h = 1$, the pole $\epsilon_p$ is less than 0, and thus $n_p$ is purely imaginary. The resulting peak can be observed in Fig. 3, where the black full line represents the MG refractive index (real and imaginary parts), which we will refer to as $n_{\mathrm{MG}}$, in terms of the imaginary part of the refractive index of particles forming a $\Phi = 14.8\%$ suspension. The $n_p$ real part has been set to zero. In the same figure, and almost overlapping with the MG predictions, are plotted blue markers; they correspond to the effective refractive index extracted by using the above-described procedure when no interaction between the particles is assumed. We denominate as branch #1 the curve formed by the blue markers. Since the volume fraction is quite low, it comes as no surprise that MG constitutes a good approximation, even though 10–15 % is usually considered as the upper limit for MG to be valid [27]. For those who would be interested in reproducing our calculations, we provide the following information: the size of the agglomerates is fixed at $R = 1.9\ \mu$m, the mean value of the number of particles contained into the 1000 realizations amounts to 1024, while the relative standard deviation between the realizations is 1.24%.

Nonetheless, the insets in the two figures evidence that MG is not in agreement with branch #1 in the vicinity of the peak. Figure 4 offers a comparison between the ensemble-averaged scattering pattern and that of a homogenous sphere whose refractive index is given by MG formula, which here gives $n_{\mathrm{MG}} = 16.27$. Obviously, the MG model is far from correctly reproducing the effective electromagnetic response of the inhomogeneous medium. We show below that the predictions given by branch #1 are also incorrect near the peak; another branch must be actually chosen in a certain segment of the $\omega_{TO}$-$\omega_{LO}$ range.

Let us enter the details of this last statement. The value $R = 1.9\ \mu$m was chosen so that the relative standard deviation is less than 2% while ensuring a manageable computing load. It must be stressed, however, that another choice for $R$ must let branch #1 unchanged, otherwise the extracted $n_{\mathrm{eff}}$ would not be consistent. We checked this point, such a condition turns out to be not fulfilled. We found that there exists a range of

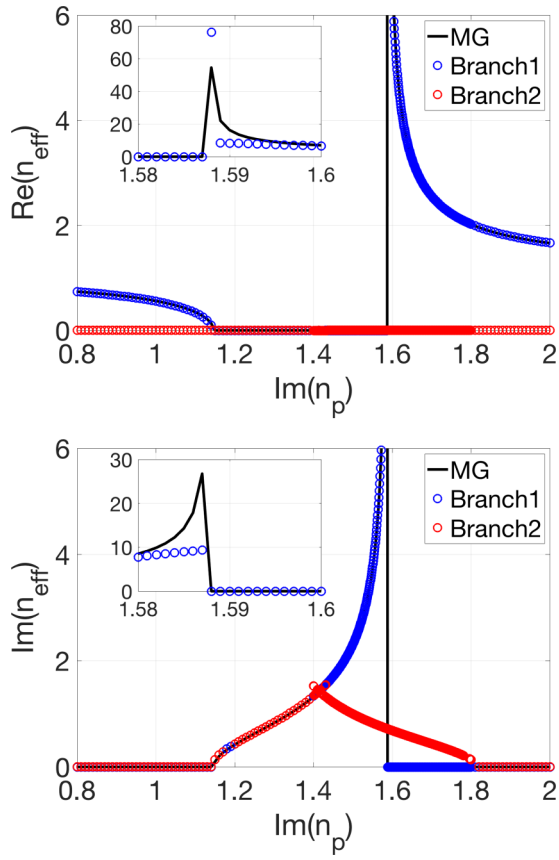


FIG. 3. Real and imaginary parts of the effective refractive index of an averaged system of agglomerates in terms of the imaginary part of the particles' refractive index. There is no interaction between the constitutive particles. The figure offers a comparison between MG's predictions and a numerical extraction, the latter leading to two set of solutions (branch #1 and branch #2). The radius of the realized spherical samples is $R = 1.9\ \mu$m.

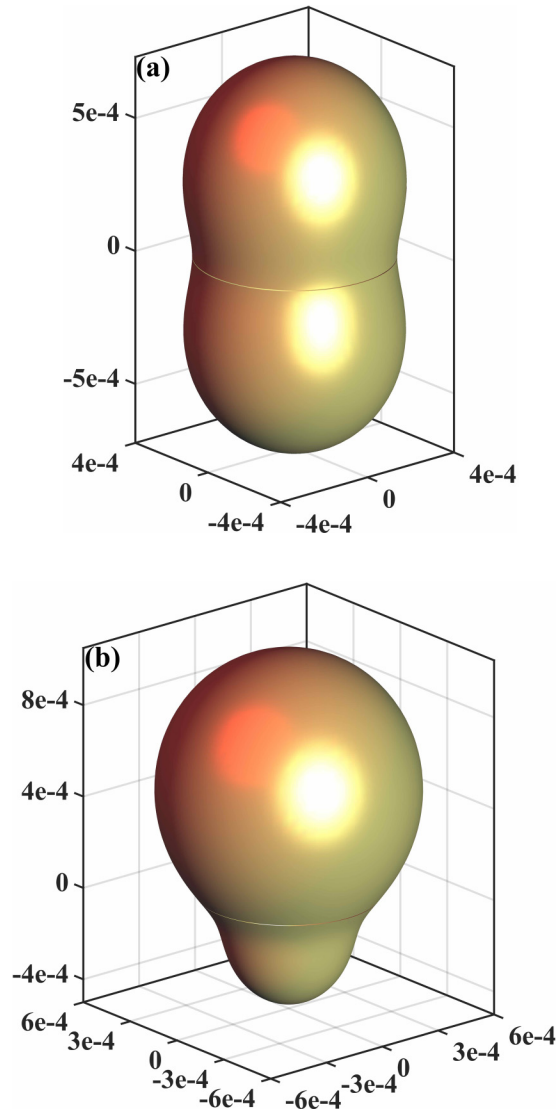


FIG. 4. Comparison of the scattering patterns of the (a) ensemble-averaged agglomerates of particles ($r_p = 100$ nm, $n_p = 1.59i$, $\Phi = 14.8\%$) and (b) homogeneous sphere with refractive index $n_{\mathrm{MG}} = 16.27$. The radius of the agglomerates is $R = 1.9\ \mu$m and the embedding medium is free space. There is no agreement between them. The scattering pattern is constructed by projecting the Poynting vector on the three spatial directions. The incident plane wave travels upward.

refractive index values for the constitutive particles in which (i) making the calculation with different $R$ modifies branch #1, and (ii) there exists another branch, which will be referred to as branch #2, that better describes the agglomerate as a homogeneous media and does not suffer from size dependance when the value of $R$ is varied. This latter branch is displayed with red dots in Fig. 3.

Qualitatively, we observe the following behavior. When the imaginary part of $n_p$ is below 1.18, only branch #1 provides correct predictions. For $\mathrm{Im}(n_p)$ ranging from 1.18–1.4, the two branches coincide. At $\mathrm{Im}(n_p) \sim 1.4$ they separate from each other; branch #2 keeps giving correct predictions while the predictions provided by branch #1 are significantly eroded until $\mathrm{Im}(n_p) \sim 1.8$. The prevalence of branch #2 over branch #1 is slight at the endpoints of the [1.4, 1.8] interval but becomes important at its center. In order to illustrate this effect, let us consider again particles with $\mathrm{Im}(n_p) = 1.59$ but forming a larger than previously considered agglomerate. Now $R = 4\ \mu$m, this means a substantial system made up of more than 10000 particles. Its scattering pattern is displayed in Fig. 5(a). With this new $R$ value, if one seeks an effective refractive index in the continuity of branch #1, the best fit yields a $n_{\mathrm{eff}}$ value that is completely different from the one obtained in Fig. 3 (where the radius was 1.9 $\mu$m). Concretely, $R = 4\ \mu$m leads to $n_{\mathrm{eff}} = 16.924$ while $R = 1.9\ \mu$m gives $n_{\mathrm{eff}} = 8.255$.

What is more, the scattering pattern of a homogeneous sphere whose refractive index is 16.924 takes the form depicted in Fig. 5(b). It is plain from the comparison of the two scattering patterns that branch #1 provides outright wrong results at $\mathrm{Im}(n_p) = 1.59$. We tried several $R$ values: they all lead to different $n_{\mathrm{eff}}$ values, and the scattering pattern of the corresponding homogeneous spheres shares no similarity with that of the suspensions of particles. Because of computation limits, we were unable to further increase $R$ in order to check if larger agglomerates would be representative of the medium

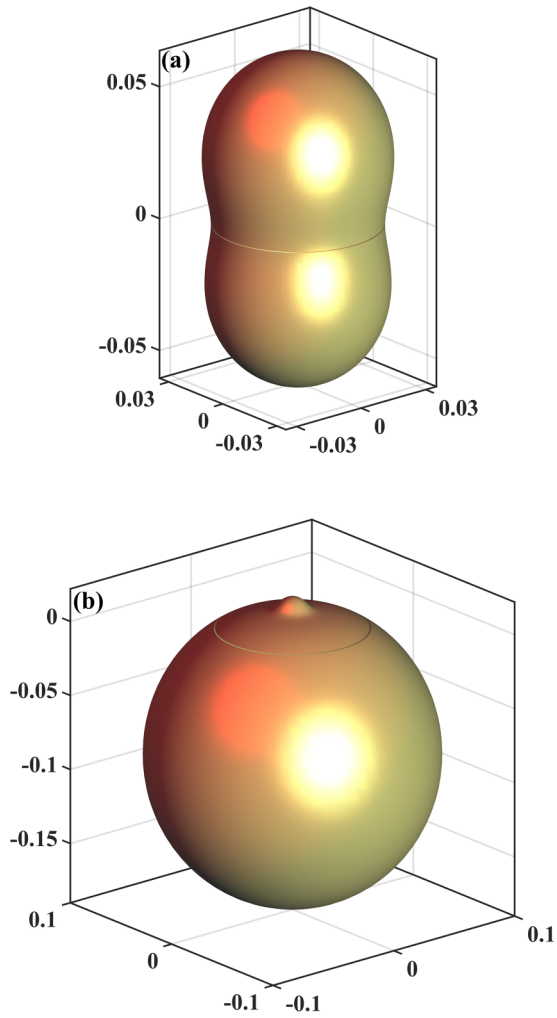


FIG. 5. Here $R = 4$ $\mu$m. Scattering patterns of the (a) ensemble-averaged agglomerates of particles and (b) homogeneous sphere with the refractive index provided by least-squares fitting: $n_{\text{eff}} = 16.924$. Obviously such an effective value does not correctly describe the inhomogeneous media.

under study and, accordingly, if one would be able to extract a stabilized and accurate $n_{\text{eff}}$ value in the continuation of branch #1. We believe that the answer is no for several reasons. First, we noticed a continuous and sensible degradation of the $n_{\text{eff}}$ predictions while $R$ was incrementally brought from 1.9 $\mu$m to 4 $\mu$m. Second, the relative standard deviation of the flux radiated by all the realizations is less than 0.5% for $R = 4$ $\mu$m, which is in agreement with Kanit's criterium for the representative volume element of an inhomogeneous medium [22].

On the other hand, looking for a solution that belongs to branch #2 provides $\text{Im}(n_{\text{eff}}) = 0.733$. The scattering patterns (not shown here) of a homogeneous sphere of radius 4 $\mu$m with this last value as refractive index is identical to that depicted in Fig. 5(a) with a precision of 0.2%. This is contrasting with the significant disparities that were found in the previous paragraph. Furthermore, the correctness of this result is strengthened by the fact that we systematically obtained the same $n_{\text{eff}}$ value when $R$ is varied.

## V. EFFECTIVE PROPERTIES OF CLUSTERS OF INTERACTING PARTICLES

In the previous section, the collective effects were neglected in the determination of the effective refractive index. The particle interactions are now taken into account by activating the higher multipolar orders.

The first concern is to determine how many multipoles are required for convergence. The contribution of higher multipoles in the $\omega_{TO}$-$\omega_{LO}$ range for some small particles was, for instance, pointed out by Gérardy [18]. However, it was sometimes claimed that a mere dipole approximation is valid in the resonant region [28]. We checked this point: higher multipoles must be definitely included to correctly model random media in the resonant region depicted in Fig. 2. By computing the power scattered by a specified agglomerate in terms of the multipolar degree, we observed strong fluctuations of the results, no convergence was achieved even at $L = 20$. This statement is verified for few particles, as in Gérardy's work, but also for large aggregates made up of several hundreds of particles. Because of the great number of required multipoles in the spectral region under study, we are facing computational complexity that prevents us from going further in the study of the effective properties. But in any case, it should be noted that the presence of resonances endows the scattered field with a strong incoherent component [29], which puts forward the question of the validity of the mean-field homogenization in the resonant region [9].

In contrast to that, the fluctuations are of less significance in those parts of the $\omega_{TO}$-$\omega_{LO}$ domain where there is no resonance. As a result, the scattering intensity plateaus by an accessible $L$ value, which typically ranges from $L = 7$, at the edges of the $\omega_{TO}$-$\omega_{LO}$ band, to $L = 12$, when getting closer to resonances. Since the simulations converge in a fairly rapid manner, the extraction of the corresponding effective properties can be achieved with the computing resources available at our laboratory. But given the large bandwidth of the resonant region, $n_{\text{eff}}$ can only be determined over a rather limited region. It appears more interesting to widen the bounds, this can be done by imposing a minimum distance between the particles.

In this context, we have already introduced a parameter, $\delta_m$, which constrains the spatial distribution of the particles with a minimum distance between them. It was plain from Fig. 2 that the extent of the resonant region depends on $\delta_m$ in such a way that the greater $\delta_m$ the narrower the resonant band. Here, we choose $\delta_m = 40$ nm, that is a distance small enough to presumptively maintain multiple scattering (we recall that $r_p = 100$ nm), while providing a larger nonresonant band in which the extraction of the effective properties is manageable. As it was done previously, $n_{\text{eff}}$ is obtained by averaging the angular diagrams of a large number of random realizations. The maximum number of realizations is now 2744. In order to understand how the effective refractive index evolves towards a given value when the agglomerates are growing, we calculate $n_{\text{eff}}$ with a number of realizations that iteratively increases from $\ell = 1$ to 2744. What is more, we make the simulations with several aggregate volumes by giving to $R$ the values 400, 700, 1000, and 1300 nm. If the volume element is representative of the material, the extracted $n_{\text{eff}}$ should not vary when the volume is further increased.

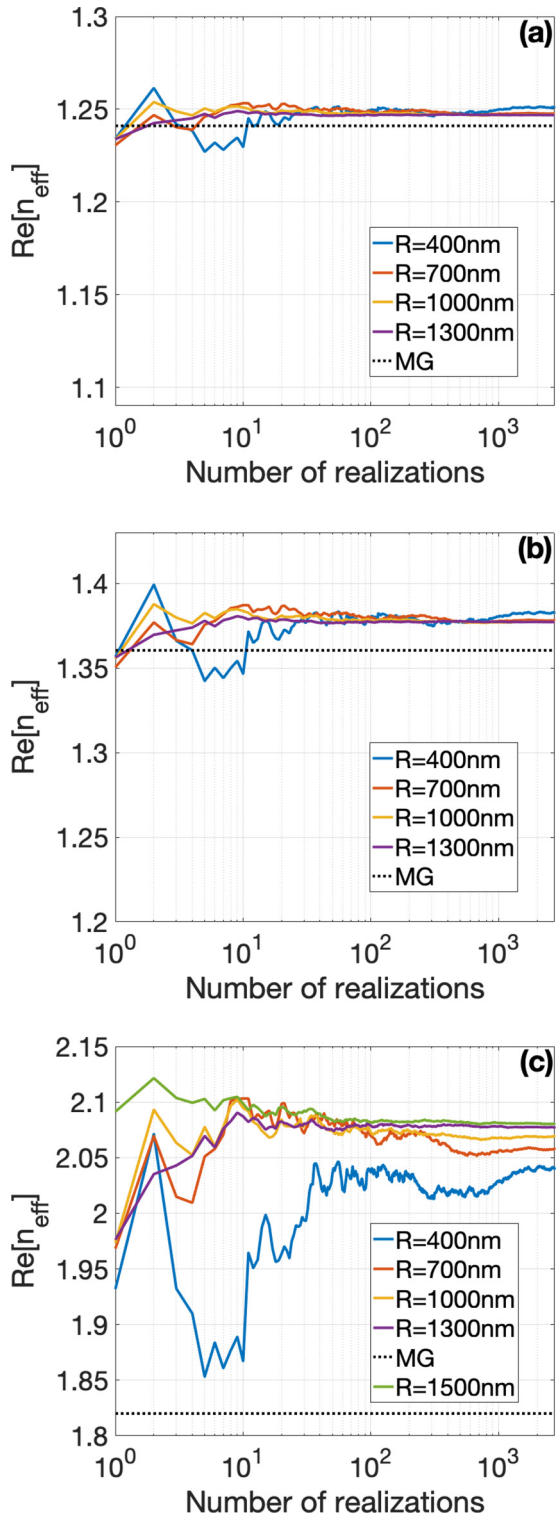


FIG. 6. Evolution of the computed effective refractive index in terms of the number of realizations in the ensemble average. Three particles' refractive indices are considered: (a) $n_p = 9.950i$, (b) $n_p = 2.845i$, and (c) $n_p = 1.883i$. For each composition, the calculation is performed with different volume sizes.

In Fig. 6, the effective refractive index, or more precisely its evolution, is shown for three values of $n_p$ belonging to the $\omega_{TO}$-$\omega_{LO}$ band. Note that the plot has a logarithmic scale for the $x$ axis and a linear scale for the $y$ axis. First, let us consider Fig. 6(a), which corresponds to $n_p = 9.950i$, i.e., far away from the resonances but still in the $\omega_{TO}$-$\omega_{LO}$ range. For either $R = 1000$ nm and $R = 1300$ nm, it can be observed that $n_{\text{eff}}$ tends to values that are, to a large extent, indistinguishable from each other. This indicates that we have converged towards the materials representative effective refractive index, which here turns out to be $n_{\text{eff}} = 1.247$. For $R = 700$ nm, the convergence is less rapid and the converged value, 1.248, is slightly different. In this context, it was evidenced by Kanit that the microstructures' volume can be reduced if counterbalanced by a greater number of realizations [22]. However, there is a lower bound below which a bias in the extraction of the effective properties is observed. Here, we clearly observed this bias when $R = 400$ nm. But depending on the required precision, the result is actually not so bad if one takes account of the reduced number of the constitutive particles, no more than 10 in this case (see Fig. 1).

The value predicted by the Maxwell-Garnett's model—here $n_{\text{MG}} = 1.241$—is also plotted in Fig. 6(a) using a black dotted line. It displays a good agreement with the calculated $n_{\text{eff}}$.

In order to put the $\omega_{TO}$-$\omega_{LO}$ range through further scrutiny, we realized another series of simulations (not shown here) assuming the same geometrical microstructures but the refractive index of the particles takes now purely real values, as it is typically done in the literature [8,16]. We tested $n_p = 2$ and $n_p = 6$, for both cases the extracted $n_{\text{eff}}$ and $n_{\text{MG}}$ deviate from each other by a slight magnitude, comparable to what we obtained when $n_p = 9.950i$. Nevertheless we found a noticeable difference regarding the volume bias: with conventional refractive indices, such as $n_p = 2$ or $n_p = 6$, the converged effective refractive index is reached for smaller volumes in comparison to the $\omega_{TO}$-$\omega_{LO}$ band.

At $n_p = 9.950i$, we were at the edge of the $\omega_{TO}$-$\omega_{LO}$ domain. Let us next examine Figs. 6(b) and 6(c) for which the refractive index of the particles are $n_p = 2.845i$ and $1.883i$, respectively. The main observation when approaching, this way, resonances is the accentuated discordance between the simulated $n_{\text{eff}}$ and $n_{\text{MG}}$, with more than 10% difference for the latter value of $n_p$. This deviation evidences a failure of the MG model in the $\omega_{TO}$-$\omega_{LO}$ band, although the subwavelength particles are nonresonant at this stage. Furthermore, it can be noticed that the bias in the $n_{\text{eff}}$ calculation is quite reluctant to the enlargement of the agglomerates at $n_p = 1.883i$; we had to realize an additional ensemble average using $R = 1500$ nm to get a converged effective value. This effect becomes stronger as we approach the resonant region.

For the sake of completion, the question of self-averaging is verified on the volume fraction of the ensembles, that is an additive property of the system [22]. To do so, we plot in Fig. 7 the deviation of the cumulative volume fraction from the targeted $\Phi = 14.8\%$ exhibited by the composite medium. The calculation is performed for several sizes of agglomerates. We can observe a convergence of the volume fraction after a certain number of realizations. As expected, the larger the agglomerates, the faster the convergence, while the precision is better by employing larger agglomerates. Furthermore, it can be verified in Fig. 7 that after 2744 realizations, self-averaging is satisfied inside a 1% precision for all the sizes that have been considered. Therefore, the fluctuations observed in Fig. 6

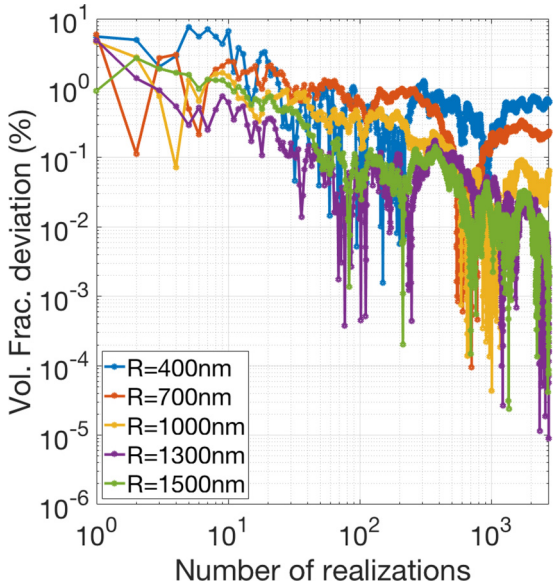


FIG. 7. Cumulative deviation of the volume fraction from the targeted one in terms of the number of realizations in the ensemble.

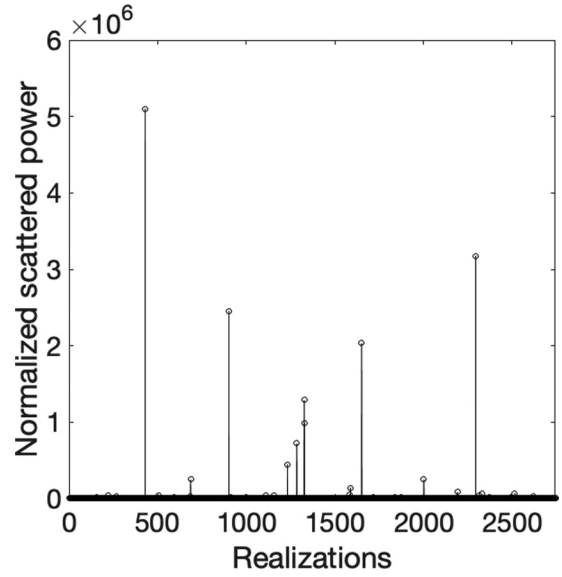


FIG. 8. Individual scattered power by 2744 different realizations. $R = 700$ nm, $n_p = 1.780i$. The result is normalized by the power scattered by the same systems of particles but under the single scattering assumption.

are not due to self-averaging issues. They are due to collective effects that are analyzed below.

In the previous section, we characterized the statistical representativity of the numerical calculations by means of the relative standard deviation, $C_V$, of the flux diffracted by all the spatial distributions. Since we were dealing with single scattering particles, the standard deviation was entirely conveyed by the fluctuations of the number of particles in each agglomerates. This is no longer true if the interactions between the scatterers are taken into account. The first three lines of Table I provide the relative standard deviation for the configurations that have been considered in this section. The observed general behavior is that a better representativeness is obtained when the volume is increased. In addition, we observe that $C_V$ increases while getting closer to the resonances, which is a signature of stronger interactions between the particles.

The last line of the table corresponds to particles whose refractive index is $n_p = 1.780i$. It evidences massive fluctuations in the total power scattered by the 2744 realizations. Such fluctuations are represented in Fig. 8 where the scattered power for all the realizations is displayed. Note that we normalized the scattered power by that scattered by the same textures assuming no interactions between the particles. Some realizations strongly resonate, with a diffracted flux that can surpass their single scattering counterparts by six orders of magnitude. This explains the unusual standard deviation at $n_p = 1.780i$. What is more, for such resonant multipolar interactions, a slight modification of parameters such as $n_p$ or $\lambda$ leads to a strong modification of the electromagnetic behavior. A minor modification of textural parameters yields the same observation: we found that a resonant agglomerate made up of more than 1000 particles can stop resonating if only one particle is removed or shifted.

TABLE I. Relative standard deviation of the realizations of the averaged system [%].

| | 400 nm | 700 nm | 1100 nm | 1300 nm |
|---|---|---|---|---|
| $n_p = 9.950i$ | 32.0 | 12.4 | 6.6 | 4.1 |
| $n_p = 2.845i$ | 32.4 | 12.6 | 6.7 | 4.2 |
| $n_p = 1.883i$ | 36.7 | 15.0 | 8.5 | 5.6 |
| $n_p = 1.780i$ | 876.0 | 765.6 | 1616.9 | 1477.9 |

Such a strong standard deviation prevents us from extracting the effective properties of the inhomogeneous media at $n_p = 1.780i$. Even if this statement is intuitive (strong fluctuations seeming incompatible with homogenization), it is however worth analyzing it at the light of the separation of the scattered field into mean and fluctuating components. Since the electromagnetic response is sensitive to the spatial distributions of the particles, the field is expected to be highly incoherent when resonances are likely to happen. Therefore, the effective properties should be derived from the mean scattered field $\langle \mathbf{E_{sc}} \rangle$, whose propagation inside the equivalent homogeneous medium is governed by Helmholtz equation [30]

$$\nabla \times \nabla \times \langle \mathbf{E_{sc}} \rangle - k_{\text{eff}}^2 \langle \mathbf{E_{sc}} \rangle = 0, \tag{4}$$

where $k_{\text{eff}} = \frac{\omega}{c} n_{\text{eff}}$. Despite that, the extraction of $n_{\text{eff}}$ has, so far, relied on the average

$$\langle \mathbf{S}_{\text{tot}} \rangle = \langle \mathbf{E_{sc}} \times \mathbf{H}_{\mathbf{sc}}^{*} \rangle \tag{5}$$

over many realizations (2744 here) of the total Poynting vector $\mathbf{S}_{\text{tot}}$. In Eq. (5), $\mathbf{E_{sc}}$ and $\mathbf{H_{sc}}$ are the whole scattered electric and magnetic fields, respectively, while the symbol $^*$ stands for complex conjugate. In agreement with Eq. (4), the quantity at stake in the comparison of the inhomogeneous and homogeneous volumes should be an averaged Poynting vector constructed from the coherent electromagnetic fields

$$\langle \mathbf{S}_{\text{coh}} \rangle = \langle \mathbf{E_{sc}} \rangle \times \langle \mathbf{H}_{\mathbf{sc}}^{*} \rangle. \tag{6}$$

TABLE II. Incoherent to coherent ratio [%].

| | 400 nm | 700 nm | 1100 nm | 1300 nm |
|---|---|---|---|---|
| Sing. Scatt. | 2.48 | 0.34 | 0.11 | 0.05 |
| $n_p = 9.950i$ | 2.63 | 0.37 | 0.12 | 0.05 |
| $n_p = 2.845i$ | 2.81 | 0.40 | 0.13 | 0.06 |
| $n_p = 1.883i$ | 4.76 | 0.86 | 0.29 | 0.14 |
| $n_p = 1.780i$ | 214.31 | 542.03 | 3878.82 | 17105.81 |

Naturally, if the incoherent field

$$\delta\mathbf{E_{sc}} = \mathbf{E_{sc}} - \langle\mathbf{E_{sc}}\rangle \tag{7}$$

is negligible, the quantities given by Eq. (5) and Eq. (6) are equivalent. But since the standard deviation is strong at $n_p = 1.780i$, $\delta\mathbf{E_{sc}}$ is expected to be important.

In order to evaluate the radiative weight of the incoherent fields, we calculate the total and coherent radiant flux across a closed surface $A$ located in the far-field region,

$$P_{\text{tot}} = \oiint \langle\mathbf{S}_{\text{tot}}\rangle d\mathbf{A} \tag{8}$$

and

$$P_{\text{coh}} = \oiint \langle\mathbf{S}_{\text{coh}}\rangle d\mathbf{A}, \tag{9}$$

which allow us to define the ratio that evaluates the preponderance of one of the coherent/incoherent components over the other:

$$\frac{P_{\text{incoh}}}{P_{\text{coh}}} = \frac{P_{\text{tot}} - P_{\text{coh}}}{P_{\text{coh}}}. \tag{10}$$

Table II displays the evaluation of such a ratio for $n_p = 9.950i$, $2.845i$, $1.883i$, and $1.780i$ in terms of the ensemble's radius. It reports as well, in the first line of the table, the evolution of the ratio in the single scattering regime. The aim of giving information related to single scattering regime is to distinguish the incoherency resulting from the bare random position of the particles in the agglomerates and that generated by the electromagnetic interactions. The former is observed in any suspension and tends to vanish as the volume is increased, while the latter is an additional component that, we will see just after, dramatically intensifies near and at resonance.

For the first three values, the incoherent component of the field is negligible compared to its coherent counterpart, in particular when the volume of the agglomerates increases. As a result, it was safe to extract the effective properties from Eq. (5), as it was done so far. Furthermore, since the independent scattering assumption and the case $n_p = 9.950i$ and $2.845i$ furnish almost the same result, we can assert that the incoherency is merely the outcome of the textural constitution of the agglomerates. It is no longer true for $n_p = 1.883i$, meaning that the interactions become significant.

Radically different is the last line of the table, which shows that resonances cause a striking enhancement of the incoherent fields at $n_p = 1.780i$. It is thus impossible to find a homogeneous sphere that behaves as the inhomogeneous sphere for $n_p = 1.780i$, and more generally for a certain range of $n_p$ values. Referring to Fig. 2, the large incoherent scattering phenomenon encompasses partially the $\omega_{TO}$-$\omega_{LO}$ domain. For $\delta_m = 40$ nm this corresponds to $\text{Im}(n_p)$ ranging approximately from 1–1.8, values for which the considered ensembles are not homogenizable, as long as $\text{Re}(n_p) \ll 1$.

TABLE III. Comparison with other effective models and approximation.

| | $n_p = 9.950i$ | $n_p = 2.845i$ | $n_p = 1.883i$ |
|---|---|---|---|
| Multipoles | 1.247 | 1.377 | 2.080 |
| Dipoles | 1.170 | 1.254 | 1.950 |
| MG | 1.241 | 1.360 | 1.820 |
| Brugg. | 1.369 | 1.328+0.499$i$ | 1.052+0.474$i$ |
| Lichn. | 1.186+0.982$i$ | 0.976+0.387$i$ | 0.933+0.288$i$ |
| Felderh. | 1.257 | 1.432 | 1.674+0.556$i$ |

## VI. COMPARISON WITH EFFECTIVE MEDIUM THEORIES; PHYSICAL APPLICATIONS; EFFECT OF LOSSES

The effective properties of the configurations depicted in Fig. 1 were obtained by numerically solving Maxwell's equations. We have evidenced that a certain number of multipoles are required in the expansion of the electromagnetic fields. Furthermore, we have shown that MG's predictions become unreliable in the $\omega_{TO}$-$\omega_{LO}$ range. Table III offers further comparisons; first with the predictions given by the models of Bruggeman [6], Lichtenecker (assuming $\alpha = 1/3$) [31], and Felderhof [32], and second with a numerical calculation where the higher multipole orders are neglected, i.e., in the approximation of the dipole-dipole interactions. As expected for the considered textures, the exact values (multipoles) fall between MG and Felderhof's predictions, at least for $n_p = 9.95i$ and $2.845i$. The Bruggeman and Lichtenecker's models lead to very different values, which is actually not surprising because the textures of the underlying materials are very different from those that are studied here. Finally, what is more interesting is that the dipole-dipole approximation offers a quite poor agreement with the actual values, making clear that higher-order multipoles carry a significant part of the electromagnetic energy.

The findings presented in this paper are relevant to several physical applications of current interest. There are many materials that are characterized by frequency ranges where the real part of the complex refractive index almost vanishes. Let us mention aluminium oxide, which is used, for instance, in paint and coatings industry or as the constituent of inhomogeneous materials employed as heat barriers. Or silica nanopowder, widely used as a polymer filler in many industrial applications due its excellent optical and electrical properties [2]. Within the $\omega_{TO}$-$\omega_{LO}$ range, the radiative properties of such kind of composite materials are highly impacted by the shape and the spatial distribution of the particles that are located near the surface of the sample. An accurate evaluation of their effect needs an exact evaluation of Maxwell's equations.

In addition, our investigation paves the way for fundamental progresses in the realm of Bergman's theory of the dielectric constant [33]. The spectral density introduced by

Bergman contains all the microstructural information of an inhomogeneous media. This means, for instance, that the effective properties of a composite can be readily predicted at any frequency, provided its spectral density is known. At our laboratory, we use the general framework of Bergman's effective medium theory and the solution of Maxwell's equations to retrieve the spectral density function and optical properties of numerical replicas of composites. This enables the extraction of the volume fraction, complex effective refractive index, and composition of phase-separated droplets in glass ceramic materials, such as those presented in Ref. [23]. However, it turns out that the spectral density strongly depends on the electromagnetic interactions in the $\omega_{TO}$-$\omega_{LO}$ range [34,35]. We have shown here that these interactions are complex and involve resonances, it is therefore crucial to better understand this regime.

In the previous paragraph, it was pointed out that assuming no loss for the particles is relevant to understand the impact of the spatial structuration of matter on its optical and electrical properties. However, since no realistic systems satisfy such assumption, it is worth analyzing the effect of losses. Let us consider an ensemble of agglomerates whose radius is $R = 700$ nm. The constitutive particles can now be lossy, we choose their refractive indices to be $n_p = x + 1.5i$. The imaginary part is a value that typically leads to strong resonances (see Fig. 2). The real part $x$ allows us to introduce nonradiative losses in the systems, in opposition to the systematic zero value that was assumed so far in the paper. In Fig. 9(a), we plot the relative standard deviation (RSD) of the flux scattered by all the realizations of the ensemble in terms of $x$ ranging from 0–1. As expected, losses eventually dissipate the resonances while the RSD is very important at $x = 0$, which is a signature of strongly resonant agglomerates, akin to the configuration depicted in Fig. 8. When the particles become lossy, the RSD is substantially decreased. However, the RSD remains significant for $x$ values that encompass realistic systems. For instance, there are frequencies for which the real part of the refractive index of silica is as low as $x = 0.05$. For this value, RSD $= 17\%$, indicating that the incoherent power remains significant.

The fact that RSD can be important even in the presence of small (but not negligible) losses should have some connection with the required multipoles. We have seen that the multipolar degree must be high if $x \sim 0$. But what if $x$ is increased? In Fig. 9(b), we have plotted the RSD in terms of the multipolar degree for several values of $x$. We can observe that at $x = 0.002$, at least four degrees are necessary to reach a proper convergence. Interestingly, realistic configurations (such as $x = 0.05$) do not satisfy the dipolar approximation (degree $= 0$) despite the size-to-wavelength ratio. Higher orders are also activated.

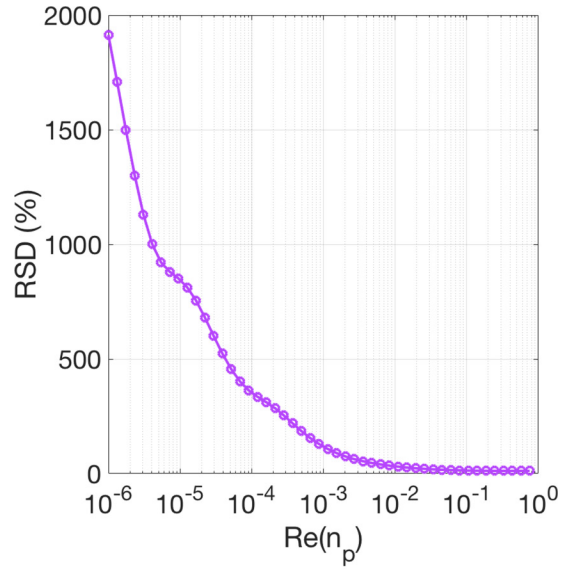


(a)

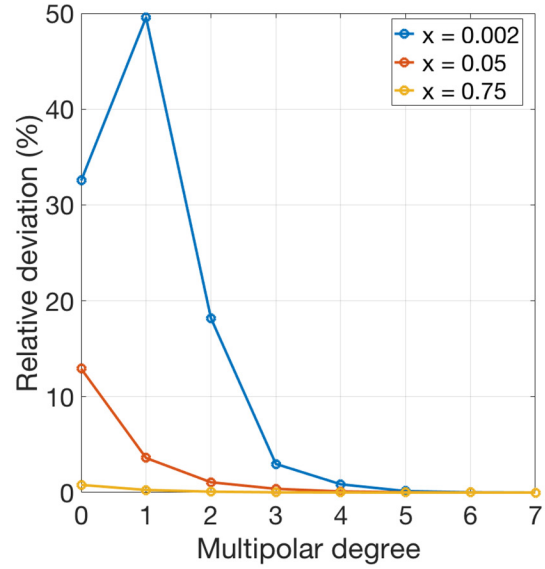


(b)

FIG. 9. (a) Relative standard deviation of the flux scattered by an ensemble of agglomerates with radius $R = 700$ nm in terms of $x$, the real part of the refractive index of the particles. (b) Relative deviation from the converged scattered flux for three values of $x$ in terms of the multipolar degree.

## VII. CONCLUSIONS

The object of this investigation was a study of the effective properties of random inhomogeneous materials near and at resonance under the influence of the incoherent scattering that happens in the $\omega_{TO}$-$\omega_{LO}$ range. The considered materials were suspensions of spherical particles that are small compared to the wavelength; the radius to wavelength ratio being $1/1000$ in most of the paper.

First, the extensive numerical calculations that were performed allowed us to examine several assertions often taken for granted, for instance the assumption of dipole-dipole interactions for small particles. The numerical technique that was employed is based on the multipolar expansion of the electromagnetic fields and, contrarily to other studies, the higher multipolar orders were not disregarded. By doing so, it was demonstrated that the system of particles exhibits resonances that can be captured only by higher multipoles, meaning that there exist configurations incorrectly modeled

if the collective effects of the particles are limited to dipole-dipole interactions. Taking these multipoles into consideration broadens the portion of the $\omega_{TO}$-$\omega_{LO}$ range where strong incoherent scattering is observed.

We proved that the bandwidth of the resonant region is directly controlled by the minimum surface-to-surface distance between the particles. It was observed that the whole $\omega_{TO}$-$\omega_{LO}$ range is susceptible to resonate if there is no restriction on the interparticle clearance, i.e., if the distribution of the particles is fully random. Nonetheless, we found that the resonant bandwidth is notably reduced if a minimum distance is imposed.

These features have a direct impact on the problem of homogenization. Since intense scattering of incoherent light is incompatible with homogenization, an ensemble of randomly distributed particles exhibits no effective properties in the spectral region bounded by $\omega_{TO}$ and $\omega_{LO}$. Between these two frequencies, homogenization is only possible if a clearance between all the particles is ensured. We showed that gradually increasing the minimum distance shrinks the resonant region, making possible the extraction of an effective refractive index in an expanding spectral domain. However, we pointed out that the incoherent component of the field keeps being quite important, which results in large deviations compared to Maxwell-Garnett's predictions.

Furthermore, we established that the number of realizations and the volume of the microstructures employed in the ensemble average are particularly sensitive in the $\omega_{TO}$-$\omega_{LO}$ range. Depending on the refractive index of the particles, the representative element volume might be substantially increased in order to ensure an accurate estimation of the effective properties. Otherwise a significant bias in the extraction is observed.

At the limit of the independent scattering regime, where there are no collective resonances anymore, the incoherent field only originates from the spatial distributions of the different averaged realizations. While it is believed that the effective properties are in plain agreement with Maxwell-Garnett in this case, it is demonstrated in this paper that such effective medium theory fails to represent agglomerates over a significant range of the particles' permittivities. We found that the effective refractive index is given by another branch.

## ACKNOWLEDGMENTS

This work is part of the OUTWARDS Project (ID: ANR-19-CE05-0021), funded by the Agence Nationale de la Recherche (ANR). The authors acknowledge François Vivet for helpful support regarding the management of CEMHTI's computing resources.

[1] R. Landauer, Electrical conductivity in inhomogeneous media, in *Electrical Transport and Optical Properties of Inhomogeneous Media*, edited by J. C. Garland and D. B. Tanner, AIP Conf. Proc. No. 40 (America Institute of Physics, New York, 1978), p. 2.

[2] A. Nzie, C. Blanchard, C. Genevois, and D. De Sousa Meneses, Retrieval of dielectric and structural properties of amorphous $Si0_2$ nanopowder based on optical measurements and Bergman's spectral representation theory, J. Appl. Phys. **126**, 104304 (2019).

[3] J. Tuoriniemi, B. Moreira, and G. Safina, Determining number concentrations and diameters of polystyrene particles by measuring the effective refractive index of colloids using surface plasmon resonance, Langmuir **32**, 10632 (2016).

[4] S. Guévelou, B. Rousseau, G. Domingues, J. Vicente, and C. Caliot, Representative elementary volumes required to characterize the normal spectral emittance of silicon carbide foams used as volumetric solar absorbers, Int. J. Heat Mass Transf. **93**, 118 (2016).

[5] J. C. M. Garnett, Colors in metal glasses and metal films, Trans. Roy. Soc. **53**, 385 (1904).

[6] D. A. G. Bruggeman, Berechnung verschiedener physikalicher konstanten von heterogenen substanzen. I. Dielektrizitatkonstanten und leitfahigkeiten der mischkorper aus isotropen substanzen, Ann. Phys. (Leipzig) **24**, 636 (1935).

[7] S. Torquato, Effective electrical conductivity of two-phase disordered composite media, J. Appl. Phys. **58**, 3790 (1985).

[8] T. E. Doyle, D. A. Robinson, S. B. Jones, K. H. Warnick, and B. L. Carruth, Modeling the permittivity of two-phase media containing monodisperse spheres: Effects of microstructure and multiple scattering, Phys. Rev. B **76**, 054203 (2007).

[9] N. J. Schilder, C. Sauvan, Y. R. P. Sortais, A. Browaeys, and J.-J. Greffet, Homogenization of an ensemble of interacting resonant scatterers, Phys. Rev. A **96**, 013825 (2017).

[10] C. Blanchard, J. A. Portí, J. A. Morente, A. Salinas, and E. Navarro, Determination of the effective permittivity of dielectric mixtures with the Transmission Line Matrix method, J. Appl. Phys. **102**, 064101 (2007).

[11] J. A. Stratton, *Electromagnetic Theory* (McGraw-Hill, New York, 1941), 1st ed.

[12] C. F. Bohren and D. R. Huffman, *Absorption and Scattering of Light by Small Particles* (John Wiley, New York, 1983).

[13] D. W. Mackowski, Calculation of total cross sections of multiple-sphere clusters, J. Opt. Soc. Am. A **11**, 2851 (1994).

[14] R. Ruppin, Effects of high-order multipoles on the extinction spectra of dispersive bispheres, Opt. Commun. **168**, 35 (1999).

[15] K. A. Fuller, Scattering and absorption cross sections of compounded spheres. I. Theory for external aggregation, J. Opt. Soc. Am. A **11**, 3251 (1994).

[16] P. Mallet, C. A. Guérin, and A. Sentenac, Maxwell-Garnett mixing rule in the presence of multiple scattering: Derivation and accuracy, Phys. Rev. B **72**, 014205 (2005).

[17] F. Bigourdan, R. Pierrat, and R. Carminati, Enhanced absorption of waves in stealth hyperuniform disordered media, Opt. Express **27**, 8666 (2019).

[18] J. M. Gérardy and M. Ausloos, Absorption spectrum of clusters of spheres from the general solution of Maxwell's equations. The long-wavelength limit, Phys. Rev. B **22**, 4950 (1980).

[19] V. A. Markel, Introduction to the Maxwell Garnett approximation: tutorial, J. Opt. Soc. Am. A **33**, 1244 (2016).

[20] J. M. Gérardy and M. Ausloos, Effects of high polar orders on the infrared absorption spectrum of ionic clusters, Surf. Sci. **106**, 319 (1981).

[21] F. Gervais and B. Piriou, Temperature dependence of transverse- and longitudinal-optic modes in $TiO_2$ (rutile), Phys. Rev. B **10**, 1642 (1974).

[22] T. Kanit, S. Forest, I. Galliet, V. Mounoury, and D. Jeulin, Determination of the size of the representative volume element for random composites: Statistical and numerical approach, Int. J. Solids Struct. **40**, 3647 (2003).

[23] S. Chenu, E. Véron, C. Genevois, G. Matzen, T. Cardinal, A. Etienne, D. Massiot, and M. Allix, Tuneable nanostructuring of highly transparent zinc gallogermanate glasses and glass-ceramics, Adv. Opt. Mater. **2**, 364 (2014).

[24] L. Martel, M. Allix, F. Millot, V. Sarou-Kanian, E. Véron, S. Ory, D. Massiot, and M. Deschamps, Controlling the size of nanodomains in calcium aluminosilicate glasses, J. Phys. Chem. C **115**, 18935 (2011).

[25] X. Chen, T. M. Grzegorczyk, B.-I. Wu, J. Pacheco, and J. A. Kong, Robust method to retrieve the constitutive effective parameters of metamaterials, Phys. Rev. E **70**, 016608 (2004).

[26] B. U. Felderhof and R. B. Jones, Spectral broadening in suspensions of metallic spheres, Z. Phys. B **62**, 43 (1985).

[27] B. A. Belyaev and V. V. Tyurnev, Electrodynamic calculation of effective electromagnetic parameters of a dielectric medium with metallic nanoparticles of a given size, J. Exp. Theor. Phys. **127**, 608 (2018).

[28] U. Felderhof and R. Jones, Multipole contributions to the effective dielectric constant of suspensions of spheres, Z. Phys. B **62**, 215 (1986).

[29] S. Jennewein, M. Besbes, N. Schilder, S. D. Jenkins, C. Sauvan, J. Ruostekoski, J.-J. Greffet, Y. R. P. Sortais, and A. Browaeys, Coherent Scattering of Near-Resonant Light by a Dense Microscopic Cold Atomic Cloud, Phys. Rev. Lett. **116**, 233601 (2016).

[30] S. Durant, O. Calvo-Perez, N. Vukadinovic, and J.-J. Greffet, Light scattering by a random distribution of particles embedded in absorbing media: Full-wave Monte Carlo solutions of the extinction coefficient, J. Opt. Soc. Am. A **24**, 2953 (2007).

[31] K. Lichtenecker, Die Dielektrizitätskonstante natürlicher und künstlicher Mischkörper, Phys. Zeitschr. **27**, 115 (1926).

[32] K. Hinsen and B. U. Felderhof, Dielectric constant of a suspension of uniform spheres, Phys. Rev. B **46**, 12955 (1992).

[33] D. J. Bergman, The dielectric constant of a composite material - A problem in classical Physics, Phys. Rep. (Sec. C Phys. Lett.) **43**, 377 (1978).

[34] J. Y. Lu, A. Raza, N. X. Fang, G. Chen, and T. Zhang, Effective dielectric constants and spectral density analysis of plasmonic nanocomposites, J. Appl. Phys. **120**, 163103 (2016).

[35] D. Zhang and E. Cherkaev, Reconstruction of spectral function from effective permittivity of a composite material using rational function approximations, J. Comput. Phys. **228**, 5390 (2009).